Supplementary information to

Encapsulation into complex coacervate core micelles promotes EGFP dimerization

Antsje Nolles, Nienke J. E. van Dongen, Adrie H. Westphal, Antonie J. W. G. Visser, J. Mieke Kleijn, Willem J. H. van Berkel and Jan Willem Borst

Index

1 Ribbon diagram of the structure of wtGFP dimer

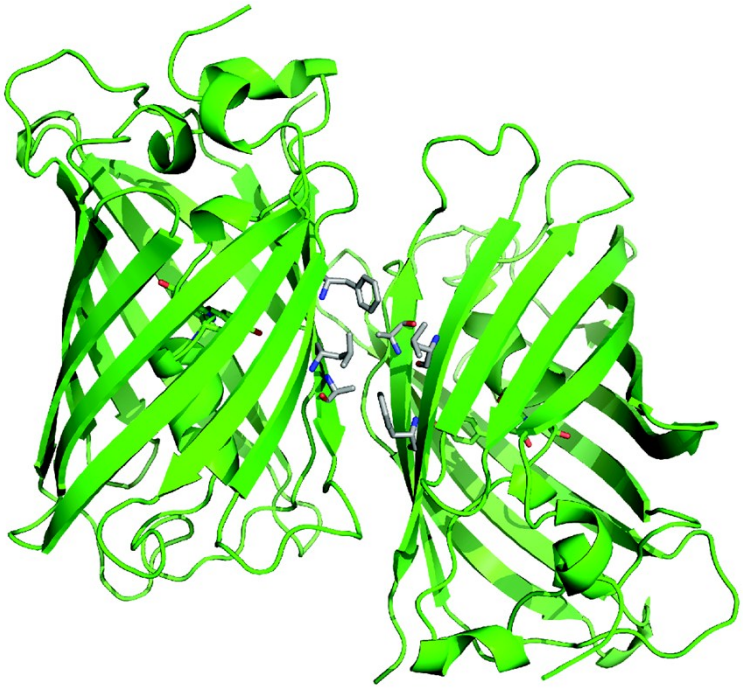

Figure S1. Ribbon diagram of the structure of wtGFP dimer. The side chains of the hydrophobic residues that are involved in dimerization (Ala206, Leu221, Phe223) are shown in gray. Cartoon based on the crystal structure of the wtGFP dimer (PDB entry 1GFL).[1]

2 PMC determination of mEGFP and SBFP2

Dynamic light scattering (DLS) measurements were performed on an ALV instrument equipped with a 300 mW Cobolt Samba-300 DPSS laser operating at 660 nm and 100 mW, and static and dynamic enhancer fiber optics for an ALV/HIGH QE APD single photon detector connected to an ALV5000/60X0 External Correlator (ALV-Laser Vertriebsgesellschaft m-b.H., Langen, Germany). The detection angle, θ, was set at 90°. For determination of the preferred micellar composition (PMC), 500 µL solutions with different polymer/protein compositions were prepared. The protein concentration was kept constant at 1 µM for each composition and the amount of P2MVP$_{41}$-*b*-PEO$_{205}$ was varied to obtain the desired values of F^+: $F^+ = [n_+]/([n_+]+[n_-])$ where $[n_+] = c_+N_+$ refers to the total concentration of positively charged groups on the polymer and $[n_-] = c_-N_-$ refers to the total concentration of negatively charged groups on the protein molecules. The number of charged groups on the diblock copolymer (N_+) taking the degree of quaternization into account, is +33.1 for P2MVP$_{41}$-*b*-PEO$_{205}$, which is used to calculate $[n_+]$. The net charge of the proteins as a function of pH was calculated using the software package PROPKA 3.1.[2, 3] The charge of the native proteins at pH 9 (N_-) is –9.87 for mEGFP and –8.96 for SBFP2, which are used to calculate $[n_-]$.

DLS autocorrelation curves were generated from 10 individual intensity traces and averaged. The inverse Laplace transformation of the average $G_2(\tau)$ ($G_2(\tau) = \langle I(t) \times I(t+\tau) \rangle / \langle I(t) \rangle^2$), performed by CONTIN software (AfterALV 1.0d, Dullware Inc., The Netherlands), was used to analyze the size distributions of the samples of encapsulated mEGFP and SBFP2 (Figure S2).[4, 5]

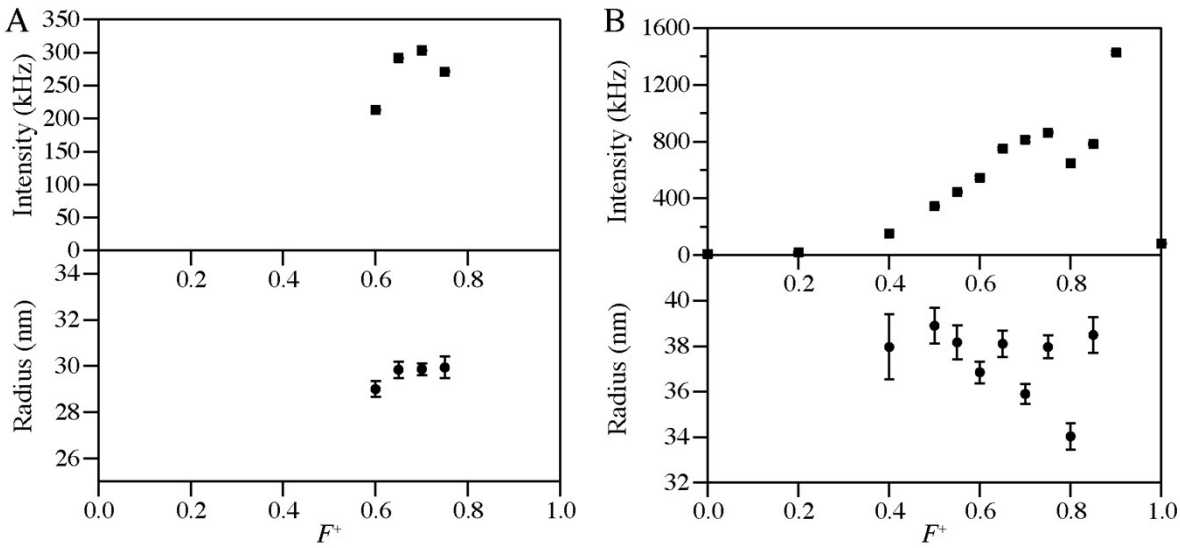

Figure S2. DLS composition experiments to determine the PMC of mEGFP and SBFP2 with $P2MVP_{41}$-*b*-PEO_{205}. Scattered intensity vs composition and hydrodynamic radius vs composition of (A) mEGFP with $P2MVP_{41}$-*b*-PEO_{205} and (B) SBFP2 with $P2MVP_{41}$-*b*-PEO_{205}. Error bars show the standard deviation of ten scans of one experiment.

3 Additional spectral analysis of EGFP

Excitation and emission spectra of 1 μM EGFP free in solution and encapsulated in C3Ms at its PMC were measured using a Cary Eclipse spectrofluorimeter (Varian Inc., Middelburg, The Netherlands). All measurements were performed at 20°C. To measure the fluorescence of state A of the encapsulated EGFP's chromophore, the two samples were excited at 390 nm and their emission spectra were recorded from 400 to 650 nm (Figure S3).

To see whether the fluorescence properties of EGFP remain the same before and after encapsulation, we measured the two samples before and after addition of NaCl (after 1 hour) with a final concentration of 0.1 M (Figure S4), with the NaCl concentration to be high enough to disintegrate the C3Ms.

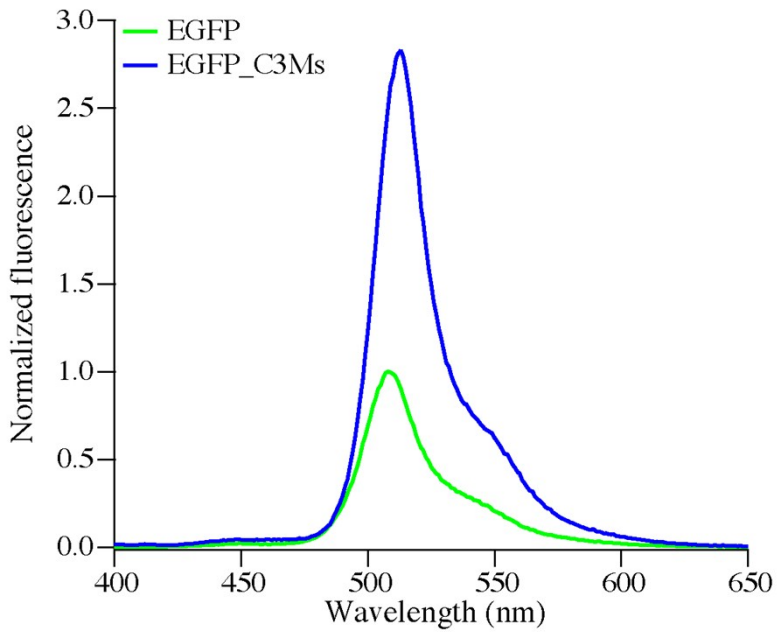

Figure S3. Normalized emission spectra of EGFP in solution (green curves) and of EGFP encapsulated in C3Ms (blue curves) after excitation at 390 nm. Spectra are normalized to the spectra of EGFP in solution.

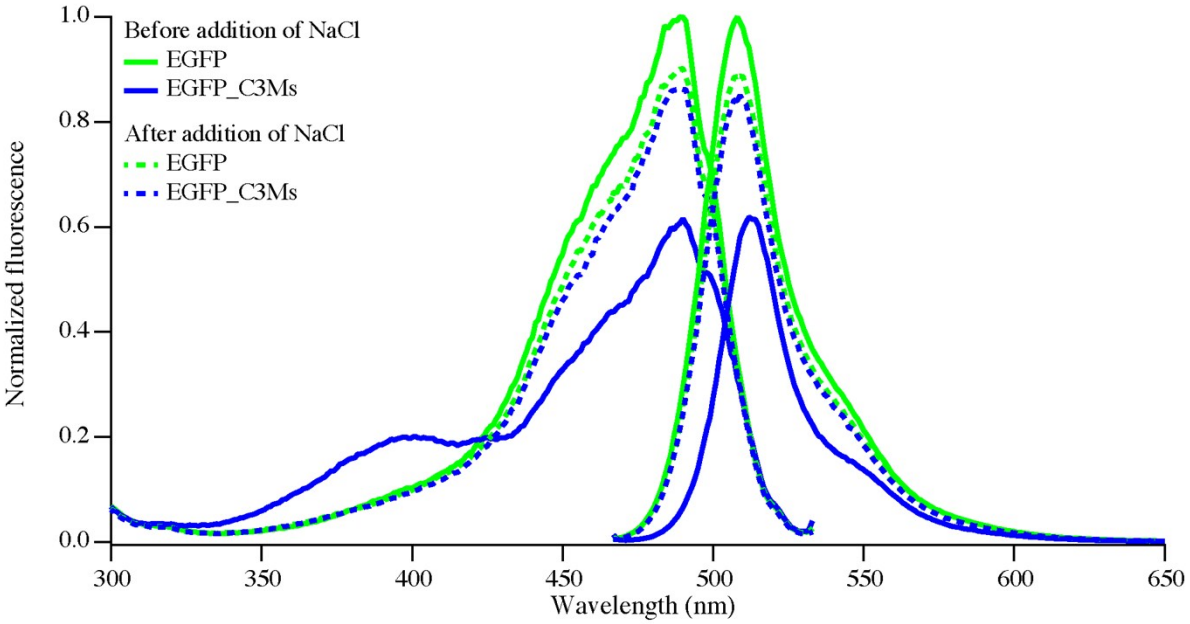

Figure S4. Normalized excitation and emission spectra of EGFP in solution (green curves) and of EGFP encapsulated in C3Ms (blue curves) before (solid line) and after (dotted line) addition of NaCl with a final concentration of 0.1 M. Spectra are normalized to the spectra of EGFP free in solution before addition of NaCl.

4 Calculation of the percentage of (m)EGFP dimers present in C3Ms

The dissociation constant (K_D) of EGFP is 0.11 mM and of mEGFP is 74 mM.[6] The dissociation/association equilibrium between dimer (D) and monomers (M) is:

$$[D] \rightleftharpoons 2[M] \tag{S1}$$

The corresponding equation for the dissociation constant is:

$$K_D = \frac{[M]^2}{[D]} \tag{S2}$$

The concentration of EGFP monomers ([M]) and dimers ([D]) is related to the total concentration (m)EGFP molecules in C3Ms ([(m)EGFP]$_{total}$) according to:

$$[\text{(m)EGFP}]_{total} = [M] + 2[D] \tag{S3}$$

Substituting Equation S3 into Equation S2 yields a quadratic equation. One of the solutions of that equation relates to the dimer concentration:

$$[D] = \frac{\left(\frac{1}{4}K_D + [\text{(m)EGFP}]_{total}\right) - \sqrt{\left(\frac{1}{4}K_D + [\text{(m)EGFP}]_{total}\right)^2 - \left([\text{(m)EGFP}]_{total}\right)^2}}{2} \tag{S4}$$

Considering a [(m)EGFP]$_{total}$ of 10 mM and the abovementioned K_D values, this results in an EGFP dimer percentage of 93% and an mEGFP dimer percentage of 18%.

5 Obtaining geometric information on the (m)EGFP molecules in C3Ms

We observed a minor decrease of the fluorescence lifetime of (m)EGFP upon encapsulation in C3Ms, which can be due to an increase of the local refractive index of the medium (n), because the refractive index squared is inversely proportional to the fluorescence lifetime of a fluorescent dye ($n^2 \propto \tau_f^{-1}$).[7, 8] The decrease in τ_f permits us to determine the refractive index of the protein-filled micelle as compared to the refractive index of water (1.33) and accounts to 1.41. However, as pointed out by Suhling and co-workers (2002)[7], it is a long-range method with a cutoff distance (at which the radiative rate constant becomes insensitive to refractive index) of about 4 μm for (m)EGFP. This would imply that not only the micellar interior, but also the micellar expanse and surrounding buffer would contribute to the refractive index. For further calculations, we will use n = 1.41, because this is the only indication we have for the refractive index in the C3Ms.

The transfer correlation times, ϕ_1, for the different ratios (m)EGFP/SBFP2 were obtained from the TRFA data and listed in Table 1. In case of homo-FRET the transfer correlation time, ϕ_1, is the reciprocal of twice the transfer rate constant, k_t, or:

$$\phi_1 = \frac{1}{2k_t} \qquad \text{(S5)}$$

in which the factor of 2 indicates the reversibility of the FRET process. The transfer rate constants are collected in Table S1. The transfer rate constant, k_t becomes larger at increasing concentrations of (m)EGFP in C3Ms. Since k_t is proportional to the transfer efficiency, encapsulated mEGFP might give more efficient homo-FRET than encapsulated EGFP.

Table S1. Transfer rate constants and distances between (m)EGFP chromophores in C3Ms with different (m)EGFP/SBFP2 ratios. For the calculation of these parameters, we used a $\kappa^2 = 0.476$, $\Phi_0 = 0.60$, $n = 1.41$ and $J = 1.01*10^{15}$ nm^4 M^{-1} cm^{-1} resulting in a $R_0 = 43$ Å. Values in parentheses are the distances between EGFP dimers, calculated with $J = 2.03*10^{15}$ nm^4 M^{-1} cm^{-1} resulting in $R_0 = 48$ Å.

Sample	k_t (ns^{-1})	R (Å)
10% EGFP in C3Ms	0.06	60 (67)
20% EGFP in C3Ms	0.14	52 (58)
30% EGFP in C3Ms	0.30	46 (51)
40% EGFP in C3Ms	0.41	43 (49)
50% EGFP in C3Ms	0.53	41 (46)
10% mEGFP in C3Ms	0.10	55
20% mEGFP in C3Ms	0.16	51
30% mEGFP in C3Ms	0.40	44
40% mEGFP in C3Ms	0.59	41
50% mEGFP in C3Ms	0.62	41

Geometric information on the (m)EGFP molecules in C3Ms can be obtained from the transfer rate constant and the Förster equation:[9, 10]

$$k_t = \frac{1}{\tau_f}\left(\frac{R_0}{R}\right)^6 \tag{S6}$$

where τ_f is the fluorescence lifetime of the donor without acceptor (2.4 ns for EGFP and 2.3 ns for mEGFP), R is the actual distance between donor and acceptor, and R_0 is the critical transfer distance or Förster distance. R_0 (in Å) can be obtained via the Förster equation (Equation S6), which requires knowledge about the orientation factor κ^2, the quantum yield of donor fluorescence (without acceptor) Φ_0, the refractive index n of the involved medium, and the spectral overlap integral J:

$$R_0 = 0.2108\left(\kappa^2 \Phi_0 n^{-4} J\right)^{1/6} \tag{S7}$$

In this case, we used a refractive index, n = 1.41, which is the best approximation for the environment of the EGFP molecules in the C3Ms. The solution in the C3Ms is more viscous than water and a corresponding orientation factor for randomized static transition dipoles should be used: κ^2 = 0.476.[11] Using these parameters, we calculated the Förster distance for a (m)EGFP FRET pair: R_0 = 43 Å (Equation S7). Now it is possible to determine the average distance, R, between the chromophores of separate (m)EGFP molecules in C3Ms by using Equation S6; these calculated average distances are listed in Table S1. In line with the expectation, for increasing ratios (m)EGFP/SBFP2 shorter average distances between the (m)EGFP chromophores are found.

From the differences in the visible-near-UV CD spectra of EGFP free in solution and encapsulated in C3Ms, we conclude that the EGFP molecules are not randomly oriented, but probably form dimers in C3Ms. In that case, the Förster radius is different. Assuming that the dimerization in C3Ms takes place in a similar way as in the crystal structure, we can obtain the initial orientation factor from the structure of dimeric EGFP from *Aequorea victoria* (PDB entry 4N3D)[12] and the transition dipole moments for the EGFP chromophore.[13] The orientation factor is quite high: κ^2 = 1.86 (Figure S5). The nearly parallel transition dipole moments would not lead to significant depolarization of fluorescence, thus EGFP homo-FRET will not be observed with TRFA. Depolarization of fluorescence with a specific transfer correlation time must then arise from homo-FRET between EGFP dimers. In a dimer, one EGFP molecule acts as donor and in the excited state it "sees" another dimer in close proximity consisting of two acceptors, making the effective extinction coefficient (and thus spectral overlap integral J) twice as large. The parameters in Equation S7 that remain the same are the refractive index (n = 1.41), the quantum yield Φ_0 and a random orientation factor κ^2 = 0.476. Taking the before mentioned changes into account, the Förster radius between two dimers would

increase to 48 Å. The average distance between the chromophores of two different dimers (they are proportional to R_0) are listed in Table S1 (values between parentheses).

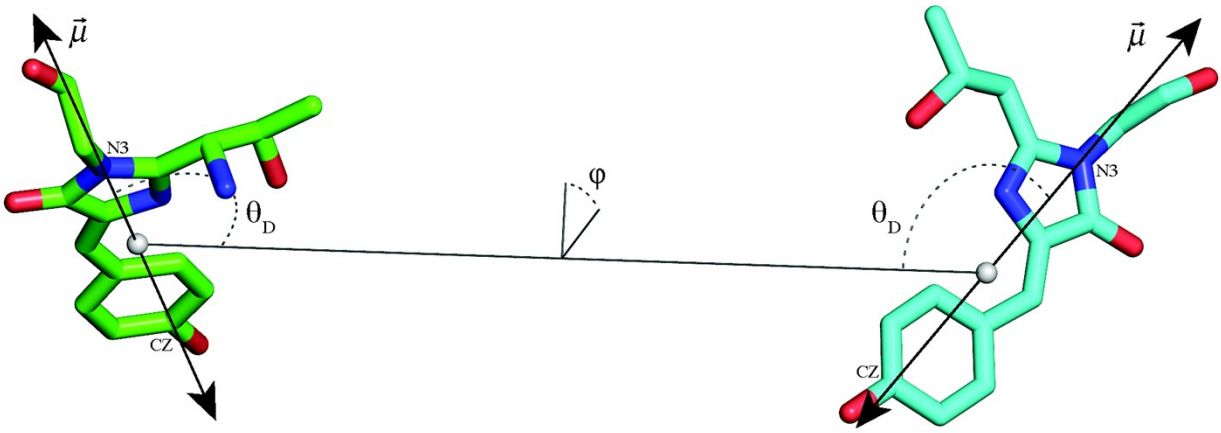

Figure S5. Illustration of the transition dipole moment, $\vec{\mu}$, of the EGFP chromophore (drawn through *N3* and *CZ* of the chromophore, based on the model of Ansbacher *et al.* (2012)[13]) with the corresponding angles between two chromophores in an EGFP dimer (based on PDB entry 4N3D[12]), which are used for the calculation of κ^2. The equation for κ^2 is: $\kappa^2 = \left(\sin\theta_D \sin\theta_A \cos\varphi - 2\cos\theta_D \cos\theta_A\right)^2$, with φ = 46.6°, θ_D = 135.6° and θ_A = 180° − θ_D = 44.4° for this EGFP dimer. This gives a κ^2 of 1.86 and a Förster radius, R_0, of 48 Å.

6 References

1. F. Yang, L. G. Moss and G. N. Phillips, *Nat. Biotechnol.*, 1996, **14**, 1246-1251.
2. M. Rostkowski, M. H. M. Olsson, C. R. Sondergaard and J. H. Jensen, *BMC Struct. Biol.*, 2011, **11**, 6.
3. M. H. Olsson, C. R. Sondergaard, M. Rostkowski and J. H. Jensen, *J. Chem. Theory Comput.*, 2011, **7**, 525-537.
4. A. Nolles, A. H. Westphal, J. A. de Hoop, R. G. Fokkink, J. M. Kleijn, W. J. H. van Berkel and J. W. Borst, *Biomacromolecules*, 2015, **16**, 1542-1549.
5. S. W. Provencher, *Comput. Phys. Commun.*, 1982, **27**, 229-242.
6. D. A. Zacharias, J. D. Violin, A. C. Newton and R. Y. Tsien, *Science*, 2002, **296**, 913-916.
7. K. Suhling, J. Siegel, D. Phillips, P. M. W. French, S. Leveque-Fort, S. E. D. Webb and D. M. Davis, *Biophys. J.*, 2002, **83**, 3589-3595.
8. K. Suhling, D. M. Davis, Z. Petrasek, J. Siegel and D. Phillips, *Proc. S. P. I. E.*, 2001, **4259**, 92-101.
9. J. W. Borst and A. J. W. G. Visser, *Meas. Sci. Technol.*, 2010, **21**, 102002.
10. N. P. Malikova, N. V. Visser, A. van Hoek, V. V. Skakun, E. S. Vysotski, J. Lee and A. J. W. G. Visser, *Biochemistry*, 2011, **50**, 4232-4241.
11. I. Z. Steinberg, *Annu. Rev. Biochem.*, 1971, **40**, 83-114.
12. N. V. Pletneva, S. V. Pletnev, A. M. Bogdanov, E. A. Goryacheva, I. V. Artemyev, E. A. Suslova, S. F. Arkhipova and V. Z. Pletnev, *Russ. J. Bioorg. Chem.*, 2014, **40**, 383-389.
13. T. Ansbacher, H. K. Srivastava, T. Stein, R. Baer, M. Merkx and A. Shurki, *Phys. Chem. Chem. Phys.*, 2012, **14**, 4109-4117.